Various carboxylates-induced eight Zn(II)/Cd(II) coordination polymers with fluorescence sensing activities for Fe(III), Cr(VI) and oxytetracycline

Yaxuan Chen, Guocheng Liu, Xiuli Wang*, Xue Lu, Na Xu, Zhihan Chang, Zhong Zhang, Xiaohui Li

College of Chemistry and Materials Engineering, Bohai University, Professional Technology Innovation Center for Conversion Materials of Solar Cell of Liaoning Province, Jinzhou, 121013, P. R. China.

Supporting Information

Materials and Methods

Synthesis of the ligand *N*,*N*′-bis (4-methylpyridine-4-yl)-2,6-naphthalene dicarboxylamide (4-bmnpd) was prepared according to the reported method.[S1] All chemical reagents and solvents are analytical grade and obtained from commercial sources without further purification. Powder X-ray diffraction (PXRD) data were collected with a D/teX super diffractometer (Cu-Kα, λ = 1.5406) at 40 kV and 40 mA over the 2θ range of 5–50º. FT-IR spectra were obtained using a Varian-640 spectrometer (KBr pellets). The thermal stability analysis was conducted at Pyres Diamond TG/DTA analyzer. The fluorescence spectra were tested with a Hitachi F-4500 fluorescence spectrometer. UV-vis absorption spectra were obtained by using a SP-1901 UV-vis spectrophotometer.

X-ray Crystallography

X-ray diffraction data of complexes **1**−**8** were collected by the φ–ω scan technique on a Bruker SMART APEX II diffractometer equipped with a CCD area detector and a graphite monochromatic Mo-Kα (λ = 0.71073 Å). Olex2 program is used to refine the data by direct method and full matrix least square method. Table 1 summarizes the crystal parameters, data collection and refinement results. Selected bond distances and bond angles are listed in Table S1–S8. Crystallographic data can be collected free of charge at www.ccdc.cam.ac.uk/conts/retrieving.html.

Preparation of 1–8

Synthesis of [Cd(4-bmnpd)(2-NBA)$_2$] (1). $CdCl_2 \cdot 2.5H_2O$ (0.0457g, 0.20 mmol), organic ligand 4-bmnpd (0.0400 g, 0.20 mmol) and 2-HNBA (0.0334 g, 0.20 mmol) were dissolved in NaOH (2 mL, 0.1 M) and H_2O (12 mL) solutions, and then placed in a 25 mL Teflon-lined autoclave under autogenous pressure at 120 °C for 4 days. When the temperature drops slowly to room temperature, the colorless block complex **1** is obtained. The yield is 17% based on 4-bmnpd. Anal. Calcd for $C_{38}H_{26}CdN_6O_{10}$: C, 54.37; H, 3.12; N, 10.02. Found: C, 55.02; H, 3.08; N, 10.04. IR (KBr, cm^{-1}): 3294m, 3078w, 2926w, 1607s, 1533s, 1416m, 1377s, 1296s, 1074w, 1026w, 826m, 741s, 694m, 534w.

Synthesis of [Cd(4-bmnpd)(3-NIP)(H_2O)] (2). The synthetic method for **2** is the same as that for **1** except that 2-HNBA is replaced by 3-H_2NIP (0.0422 g, 0.20 mmol). Colorless block complex **2** is obtained. The yield is 20% based on 4-bmnpd. Anal. Calcd for $C_{32}H_{25}CdN_5O_9$: C, 52.22; H, 3.42; N, 9.52. Found: C, 52.73; H, 3.46; N, 9.22. IR (KBr, cm^{-1}): 3300s, 3067w, 1638s, 1524s, 1425m, 1387m, 1309m, 1062w, 823m, 712m, 671w, 532w.

Synthesis of [Cd_2(4-bmnpd)(TCPA)$_2$] (3). The synthetic method for **3** is the same as that for **1** except that 2-HNBA is replaced by H_2TCPA (0.0304 g, 0.10 mmol). Colorless block complex **3** is obtained. The yield is 24% based on 4-bmnpd. Anal. Calcd for $C_{40}H_{20}Cd_2Cl_8N_4O_{10}$: C, 39.22; H, 1.65; N, 4.57. Found: C, 39.13; H, 1.56; N, 4.49. IR (KBr, cm^{-1}): 3250m, 3065w, 1618s, 1545s, 1435m, 1338s, 1290w, 1064w, 903w, 827w, 648w.

Synthesis of [Cd(4-bmnpd)(5-HIP)(H_2O)] (4). The synthetic method for **4** is the same as that for **1** except that 2-HNBA is replaced by 5-H_2HIP (0.0364 g, 0.20 mmol). Colorless block complex **4** is obtained. The yield is 27% based on 4-bmnpd. Anal. Calcd for $C_{32}H_{26}CdN_4O_8$: C,

54.37; H, 3.71; N, 7.93. Found: C, 54.53; H, 3.62; N, 7.84. IR (KBr, cm^{-1}): 3433m, 3277s, 1633s, 1568s, 1516m, 1375s, 1271m, 1066w, 931w, 889w, 779m, 735s, 609w, 538w.

Synthesis of [Cd(4-bmnpd)$_{0.5}$(5-MIP)(H$_2$O)] (5). The synthetic method for **5** is the same as that for **1** except that 2-HNBA is replaced by 5-H_2MIP (0.0360 g, 0.20 mmol). Colorless block complex **5** is obtained. The yield is 19% based on 4-bmnpd. Anal. Calcd for $C_{21}H_{18}CdN_2O_6$: C, 49.77; H, 3.58; N, 5.53. Found: C, 49.83; H, 3.62; N, 5.44. IR (KBr, cm^{-1}): 3398w, 3047w, 2928w, 1635m, 1548s, 1514s, 1427s, 1364s, 1296m, 1016w, 775s, 732m, 621w, 530w.

Synthesis of [Cd$_3$O(4-bmnpd)(1,4-PHDA)$_2$(H$_2$O)]·H$_2$O (6). The synthetic method for **6** is the same as that for **1** except that 2-HNBA is replaced by 1,4-H_2PHDA (0.0384 g, 0.20 mmol). Colorless block complex **6** is obtained. The yield is 22% based on 4-bmnpd. Anal. Calcd for $C_{44}H_{42}Cd_3N_4O_{16}$: C, 43.32; H, 3.47; N, 4.59. Found: C, 43.29; H, 3.52; N, 4.54. IR (KBr, cm^{-1}): 3381s, 3053w, 1645s, 1528s, 1427m, 1382s, 1311m, 1015m, 814w, 768m, 717m, 611w.

Synthesis of [Zn(4-bmnpd)(5-MIP)] (7). The synthetic method for **7** is the same as that for **5** except that $CdCl_2·6H_2O$ is replaced by $Zn(NO_3)_2·6H_2O$ (0.0595 g, 0.20 mmol). Colorless block complex **7** is obtained. The yield is 25% based on 4-bmnpd.Anal. Calcd for $C_{33}H_{26}ZnN_4O_6$: C, 61.93; H, 4.09; N, 8.76. Found: C, 61.89; H, 4.12; N, 8.74. IR (KBr, cm^{-1}): 3271s, 3067m, 2928w, 1647s, 1574s, 1431s, 1369s, 1368m, 1028m, 905m, 777m, 732m, 532w.

Synthesis of [Zn(4-bmnpd)(1,2,4,5-BTA)$_{0.5}$]·2H$_2$O (8). The synthetic method for **8** is the same as that for **7** except that 5-H_2HIP is replaced by 1,2,4,5-H_4BTA (0.0254 g, 0.10 mmol). Colorless block complex **8** is obtained. The yield is 19% based on 4-bmnpd. Anal. Calcd for $C_{29}H_{25}ZnN_4O_8$: C, 55.92; H, 4.05; N, 8.99. Found: C, 55.89; H, 4.02; N, 8.94. IR (KBr, cm^{-1}): 3439w, 3277s, 2787w, 1641s, 1533w, 1489w, 1368s, 806m, 707m, 613m.

IR, Powder X-ray diffraction (PXRD) and thermogravimetric (TG) analyses.

The infrared spectra of complexes **1–8** is shown in Fig. S1, and the frequency range of the test is 500 – 4000 cm^{-1}. The peak near 3396 cm^{-1} in CP **6** belongs to the water absorption peak.[S2] The vibration absorption of methylene (CH_2) in 4-bmnpd occurs near 3000 cm^{-1}.[S3] The peak value around 1390 cm^{-1} is due to the role of carboxyl group in organic carboxylic acid.[S4] The absorption peak of carbonyl group in the ligand of complex is around 1600 cm^{-1}.[S5]

X-ray diffraction of the complexes was carried out at room temperature. As shown in Fig. S2, the spectra determined by the experiment is highly consistent with the curve obtained from the simulation of single crystal data, and the positions of diffraction peaks are well consistent with the simulated results, indicating that the obtained complexes have good purity.

The TG analyses of CPs **1–8** were measured under a N_2 atmosphere in the temperature range from 30 to 800 °C. The weight loss of **1** and **7** occurred with one step while **2**–**6** and **8** occurred with two steps (Fig. S3). The weight losses ending at 235 °C, 251 °C, 238 °C, 97 °C, 189 °C and 232 °C are attributed to the loss of the lattice water molecules and/or coordinated water molecules for CPs **2**, **4**, **5**, **6** and **8**, or carboxylate for CP **3**. The subsequent weight losses occurring at 271 °C, 363 °C, 358 °C, 318 °C, 319° C, 298 °C, 322 °C and 343 °C, correspond to the decomposition of the organic components of **1**–**8**.

Details of fluorescence experiment

3 mg crystal powder was ground and soaked in cationic solution (Al^{3+}, Ba^{2+}, Ca^{2+}, Co^{2+}, Cu^{2+}, Fe^{3+}, K^+, Mg^{2+}, Na^+, Pb^{2+}, Zn^{2+}), anionic solution (NO_3^-, Br^-, HCO_3^-, I^-, Cl^-, CO_3^{2-}, OH^-, CH_3COO^-, $Cr_2O_7^{2-}$ and CrO_4^{2-}) and antibiotic (Penicillin, Amoxicillin, Dopamine, Oxytetracycline, Thiamphenicol) with the concentration of 0.01 mol L^{-1}. Ultrasonic treatment was carried out for 30 minutes, and the suspension obtained was tested for selectivity and anti-interference.

pH and thermal stability.

To investigate the stability of CPs **1**–**8**, a certain amount of CPs **1**–**8** samples were soaked in different acidic and alkaline aqueous solutions and then characterized by PXRD (Fig. S4). The experimental peaks of CPs **1**–**8** in the pH range of 3–12 were roughly consistent with the

simulated peak positions, indicating that CPs **1**–**8** exhibited better pH stability. The thermal stability of CP **5** was further studied, and PXRD patterns under 100, 200, 300, and 400 °C were obtained (Fig. S5). Compared with that at room temperature, it can be seen that the peak positions of PXRD are consistent at 300 °C, which indicates that the framework is stable up to 300 °C. The good pH stability and thermal stability provide the necessary conditions for subsequent fluorescence detection.

[S1] M. Sarka and K. Biradha, *Cryst. Growth Des.*, 2006, **6**, 202.
[S2] R. Yang, K. V. Hecke, B.Y. Yu, G. Y. Li and G. H. Cui, *Transit. Metal Chem.*, 2014, **39**, 535.
[S3] S. Shukla, A. Maithani and D. Srivastava, *Des. Monomers Polym.*, 2014, **17**, 69.
[S4] Y. T. Qin, B. W. Wang, J. Y. Li, X. C. Wu and L. G. Chen, *Transit. Metal Chem.*, 2019, **44**, 595.
[S5] B. Dolenský, R. Konvalinka, M. Jakubek and V. Král, *J. Mol. Struct.*, 2013, **1035**, 124.

Table S1 Selected bond distances (Å) and angles (°) for complex **1**.

1			
Cd(1)-N(1)	2.2765(17)	Cd(1)-N(1)	2.2765(17)
Cd(1)-N(1)A	2.2766(17)	Cd(1)-N(1)B	2.2766(17)
Cd(1)-O(1)	2.2879(15)	Cd(1)-O(1)	2.2879(15)
N(1)-Cd(1)-N(1)A	180.0	O(1)-Cd(1)-O(5)B	78.60(6)
N(1)-Cd(1)-O(1)	91.70(6)	O(1)A-Cd(1)-O(5)B	101.40(6)
N(1)A-Cd(1)-O(1)	88.30(6)	N(1)-Cd(1)-O(5)C	91.82(6)
N(1)-Cd(1)-O(1)A	88.30(6)	N(1)A-Cd(1)-O(5)C	88.18(6)
N(1)A-Cd(1)-O(1)A	91.70(6)	O(1)-Cd(1)-O(5)C	101.40(6)
O(1)-Cd(1)-O(1)A	180.0	O(1)A-Cd(1)-O(5)C	78.60(6)
N(1)-Cd(1)-O(5)B	88.18(6)	O(5)B-Cd(1)-O(5)C	180.0
N(1)A-Cd(1)-O(5)B	91.82(6)	C(10)-O(1)-Cd(1)	124.32(14)

Symmetry code for **1**: A: $-x + 1, -y + 2, -z + 1$, B: $-x + 1, -y + 1, -z + 1$, C: $x, y + 1, z$.

Table S2: Selected bond distances (Å) and angles (°) for complex **2**

2			
Cd(1)-O(1W)	2.246(4)	Cd(1)-O(2)	2.316(3)
Cd(1)-O(1)A	2.254(3)	Cd(1)-O(3)	2.343(3)
Cd(1)-N(1)	2.314(4)	Cd(1)-N(4)	2.352(4)
O(1W)-Cd(1)-O(1)A	91.25(13)	O(1W)-Cd(1)-N(1)	88.34(13)
O(1)A-Cd(1)-N(1)	99.33(13)	O(1W)-Cd(1)-O(2)	170.92(12)
O(1)A-Cd(1)-O(2)	93.36(11)	N(1)-Cd(1)-O(2)	98.62(12)
O(1W)-Cd(1)-O(3)	94.77(13)	O(1)A-Cd(1)-O(3)	170.81(12)
N(1)-Cd(1)-O(3)	87.81(11)	O(2)-Cd(1)-O(3)	79.76(11)
O(1W)-Cd(1)-N(4)	88.89(13)	O(1)A-Cd(1)-N(4)	86.54(13)
N(1)-Cd(1)-N(4)	173.56(13)	O(2)-Cd(1)-N(4)	83.58(13)
O(3)-Cd(1)-N(4)	86.63(12)		

Symmetry code for **2**: A: $-x, -y - 2, -z$.

Table S3: Selected bond distances (Å) and angles (°) for complex **3**

		3	
Cd(1)-O9A	2.311(6)	Cd(1)-N(1)	2.292(7)
Cd(1)-O(2)A	2.209(6)	Cd(2)-O(6)	2.269(6)
Cd(1)-O(1)	2.201(6)	Cd(2)-O(5)A	2.341(7)
Cd(1)-O(8)A	2.309(6)	Cd(2)-N(3)	2.290(7)
O(2)A-Cd(1)-O(9)A	100.3(2)	O(4)-Cd(2)-O(7)A	161.0(2)
O(2)A-Cd(1)-O(8)A	105.5(2)	O(4)-Cd(2)-O(6)	99.2(3)
O(2)A-Cd(1)-N1	107.1(3)	O(4)-Cd(2)-O(5)A	81.5(3)
O(1)-Cd(1)-O(9)A	104.2(2)	O(4)-Cd(2)-N(3)	104.9(3)
O(1)-Cd(1)-O(2)A	98.1(2)	O(6)-Cd(2)-O(9)A	77.7(2)
O(1)-Cd(1)-O(8)A	151.6(2)	O(6)-Cd(2)-O(7)A	92.2(2)
O(1)-Cd(1)-N(1)	100.9(3)	O(6)-Cd(2)-O(5)A	160.2(2)
O(8)A-Cd(1)-O(9)A	56.5(2)	O(6)-Cd(2)-N(3)	97.2(2)
N(1)-Cd(1)-O(9)A	139.5(2)	O(5)A-Cd(2)-O(9)A	82.6(2)
N(1)-Cd(1)-O(8)A	87.2(3)	N(3)-Cd(2)-O(9)A	168.7(2)
O(7)A-Cd(2)-O(9)A	81.7(2)	N(3)-Cd(2)-O(7)A	88.5(2)
O(7)A-Cd(2)-O(5)A	82.6(2)	N(3)-Cd(2)-O(5)A	101.8(3)
O(4)-Cd(2)-O(9)A	86.0(2)		

Symmetry code for **3**: A: –1 + *x*, *y*, *z*, B: –*x*, –1 – *y*, 1 – *z*, C: –*x*, 2 – *y*, 2 – *z*.

Table S4: Selected bond distances (Å) and angles (°) for complex **4**

		4	
Cd(1)-N(1)	2.314(3)	Cd(1)-N(3)	2.372(3)
Cd(1)-O(1)	2.322(2)	Cd(1)-O(3)A	2.471(3)
Cd(1)-O(1W)	2.335(3)	Cd(1)-O(2)	2.590(3)
Cd(1)-O(4)A	2.369(2)		
N(1)-Cd(1)-O(1)	139.26(9)	N(1)-Cd(1)-O(1W)	96.36(10)
O(1)-Cd(1)-O(1W)	85.86(10)	N(1)-Cd(1)-O(4)A	140.12(9)
O(1)-Cd(1)-O(4)A	80.27(8)	O(1W)-Cd(1)-O(4)A	90.65(10)
N(1)-Cd(1)-N(3)	85.97(10)	O(1)-Cd(1)-N(3)	89.74(10)
O(1W)-Cd(1)-N(3)	175.34(11)	O(4)A-Cd(1)-N(3)	90.11(10)
N(1)-Cd(1)-O(3)A	87.24(9)	O(1)-Cd(1)-O(3)A	133.48(9)
O(1W)-Cd(1)-O(3)A	88.06(11)	O(4)A-Cd(1)-O(3)A	53.71(8)
N(3)-Cd(1)-O(3)A	96.10(10)	N(1)-Cd(1)-O(2)	86.60(9)
O(1)-Cd(1)-O(2)	52.72(8)	O(1W)-Cd(1)-O(2)	88.53(11)
O(4)A-Cd(1)-O(2)	132.93(8)	N(3)-Cd(1)-O(2)	87.59(10)
O(3)A-Cd(1)-O(2)	172.59(8)		

Symmetry code for **4**: A: *x*, *y* + 1, *z*.

Table S5: Selected bond distances (Å) and angles (°) for complex **5**

5			
Cd(1)-O(1W)	2.27(2)	Cd(1)-N(1)	2.343(2)
Cd(1)-O(1)	2.27(2)	Cd(1)-O(4)B	2.40(2)
Cd(1)-O(5)A	2.30(2)	Cd(1)-O(3)B	2.42(2)
Cd(1)-O(2)	2.65(2)		
O(1W)-Cd(1)-O(1)	93.4(9)	O(1W)-Cd(1)-O(5)A	86.3(9)
O(1)-Cd(1)-O(5)A	136.5(9)	O(1W)-Cd(1)-N(1)	164.5(10)
O(1)-Cd(1)-N(1)	85.6(9)	O(5)A-Cd(1)-N(1)	83.9(9)
O(1W)-Cd(1)-O(4)B	105.4(9)	O(1)-Cd(1)-O(4)B	82.7(8)
O(5)A-Cd(1)-O(4)B	139.1(8)	N(1)-Cd(1)-O(4)B	89.8(9)
O(1W)-Cd(1)-O(3)B	97.5(9)	O(1)-Cd(1)-O(3)B	137.1(9)
O(5)A-Cd(1)-O(3)B	85.7(8)	N(1)-Cd(1)-O(3)B	93.7(9)
O(4)B-Cd(1)-O(3)B	54.4(7)		

Symmetry code for **5**: A: $-x, -y + 1, -z + 1$, B: $x, y + 1, z$.

Table S6: Selected bond distances (Å) and angles (°) for complex **6**

6			
Cd(1)-O(5)	2.242(3)	Cd(1)-O(2)B	2.354(3)
Cd(1)-O(3)	2.250(3)	Cd(1)-N(1)	2.359(4)
Cd(1)-O(5)A	2.298(3)	Cd(1)-O(1W)	2.418(4)
Cd(2)-O(5)	2.290(3)	Cd(2)-O(2)F	2.312(4)
Cd(2)-O(5)D	2.290(3)	Cd(2)-O(4)A	2.323(3)
Cd(2)-O(2)E	2.312(4)	Cd(2)-O(4)G	2.323(3)
O(5)-Cd(1)-O(3)	173.87(12)	O(5)-Cd(2)-O(5)D	180.0
O(5)-Cd(1)-O(5)A	81.24(11)	O(5)-Cd(2)-O(2)E	103.99(11)
O(3)-Cd(1)-O(5)A	98.41(11)	O(5)D-Cd(2)-O(2)E	76.01(11)
O(5)-Cd(1)-O(2)B	102.62(12)	O(5)-Cd(2)-O(2)F	76.01(11)
O(3)-Cd(1)-O(2)B	83.13(13)	O(5)D-Cd(2)-O(2)F	103.99(11)
O(5)A-Cd(1)-O(2)B	75.03(11)	O(2)E-Cd(2)-O(2)F	180.0
O(5)-Cd(1)-N(1)	96.54(12)	O(5)-Cd(2)-O(4)A	94.04(11)
O(3)-Cd(1)-N(1)	84.71(12)	O(5)D-Cd(2)-O(4)A	85.96(11)
O(5)A-Cd(1)-N(1)	171.20(12)	O(2)E-Cd(2)-O(4)A	89.95(12)
O(2)B-Cd(1)-N(1)	97.29(13)	O(2)F-Cd(2)-O(4)A	90.05(12)
O(5)-Cd(1)-O(1W)	94.82(13)	O(5)-Cd(2)-O(4)G	85.96(11)
O(3)-Cd(1)-O(1W)	79.04(14)	O(5)D-Cd(2)-O(4)G	94.04(11)
O(5)A-Cd(1)-O(1W)	87.54(11)	O(2)E-Cd(2)-O(4)G	90.05(12)
O(2)B-Cd(1)-O(1W)	152.92(13)	O(2)F-Cd(2)-O(4)G	89.95(12)
N(1)-Cd(1)-O(1W)	101.16(13)	O(4)A-Cd(2)-O(4)G	180.00(9)

Symmetry code for **6**: A: –*x* + 1, –*y* + 2, –*z* + 1, B: *x*, –*y* + 3/2, *z* – 1/2, C: *x* + 1, *y*, *z*, D: –*x*, –*y* + 2, –*z* + 1, E: *x* – 1, –*y* + 3/2, *z*−1/2, F: –*x* + 1, *y*+1/2, –*z* + 3/2, G: *x* – 1, *y*, *z*

Table S7: Selected bond distances (Å) and angles (°) for complex **7**

		7	
Zn(1)–O(1)	1.959(3)	Zn(1)–O(4)A	1.988(4)
Zn(1)–N(1)	2.066(4)	Zn(1)–N(4)B	2.087(4)
O(1)–Zn(1)–O(4)A	99.30(15)	O(1)–Zn(1)–N(1)	106.92(16)
O(4)A–Zn(1)–N(1)	126.52(17)	O(1)–Zn(1)–N(4)B	110.01(16)
O(4)A–Zn(1)–N(4)B	105.87(16)	N(1)–Zn(1)–N(4)B	107.46(16)

Symmetry code for **7**: A: *x* + 1, *y* + 1, *z*, B: –*x* + 2, –*y* + 1, –*z* + 1.

Table S8: Selected bond distances (Å) and angles (°) for complex **8**

		8	
Zn(1)-O(4)	1.9235(16)	Zn(1)-N(2)	2.026(2)
Zn(1)-O(2)A	1.9305(17)	Zn(1)-N(1)B	2.053(2)
O(4)-Zn(1)-O(2)A	118.07(8)	O(4)-Zn(1)-N(1)B	110.11(8)
O(4)-Zn(1)-N(2)	117.87(8)	O(2)A-Zn(1)-N(1)B	95.86(8)
O(2)A-Zn(1)-N(2)	106.33(8)	N(2)-Zn(1)-N(1)B	105.81(8)

Symmetry code for **8**: −*x* + 3, −*y* + 2, −*z* + 2, B: −*x* + 1, −*y*, −*z* + 1.

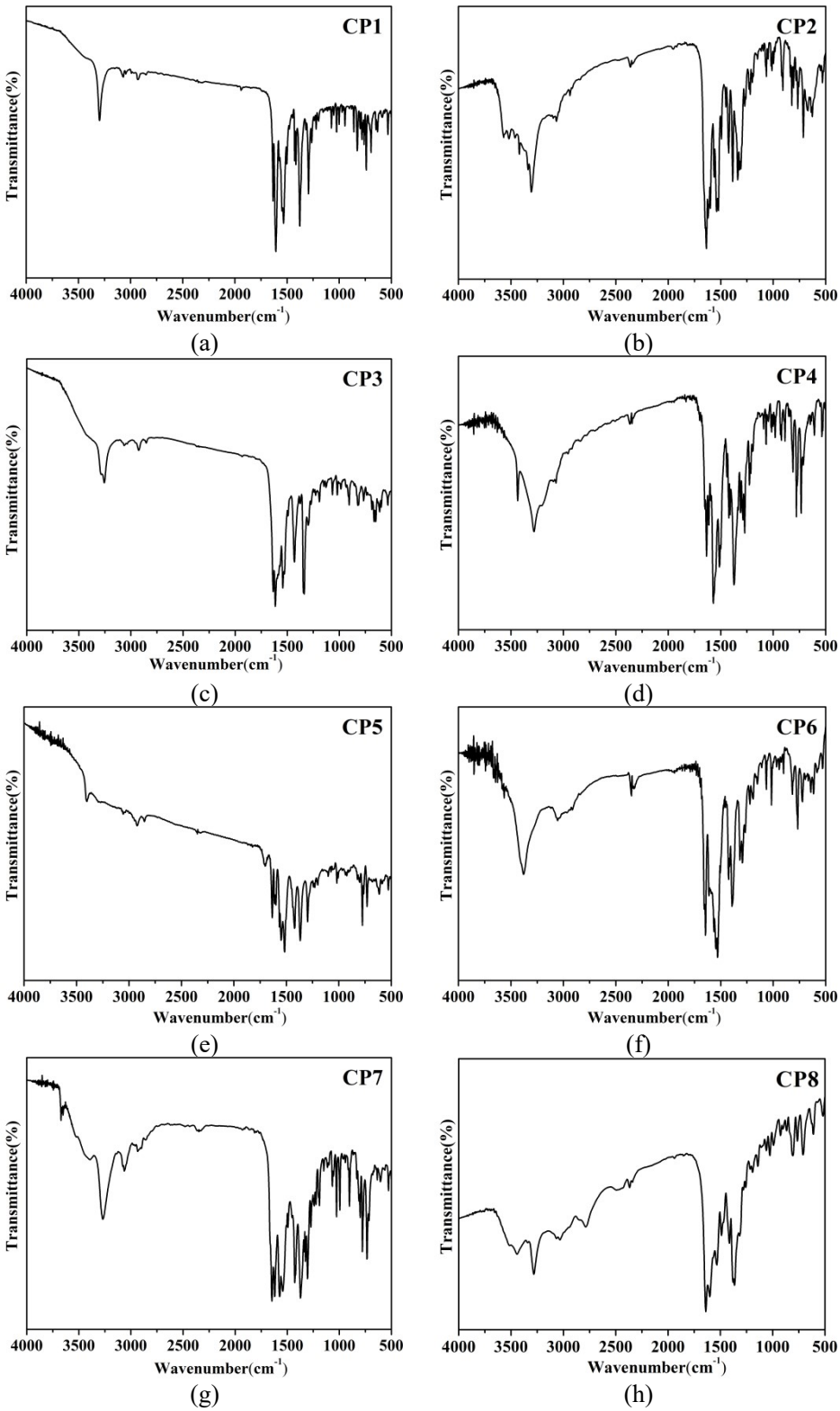

Fig. S1 The IR spectra of CPs **1**–**8**.

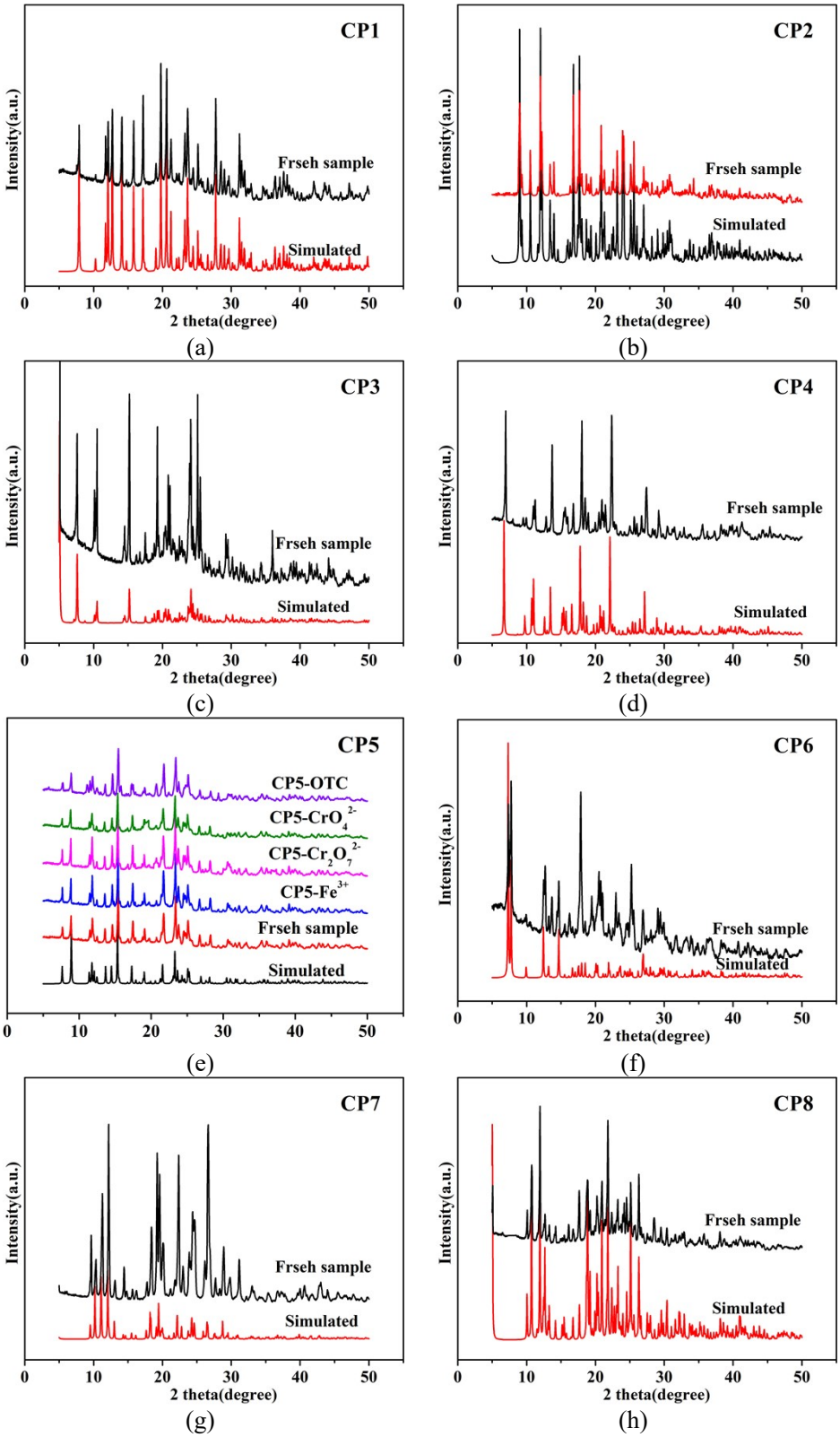

Fig. S2 The PXRD patterns of simulated and fresh samples for **1**–**8** (a-h) and the PXRD patterns of CP 5 after being soaked in different solutions (e).

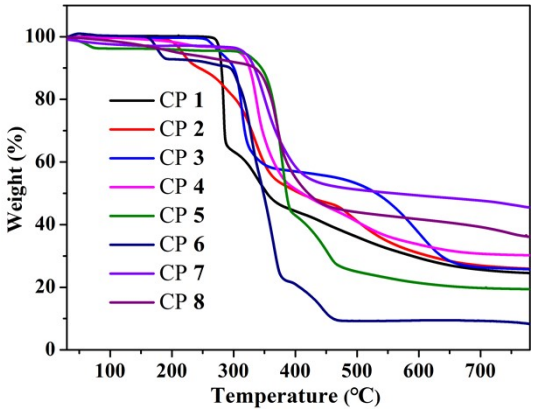

Fig. S3 The TG curves of CP **1**–**8**.

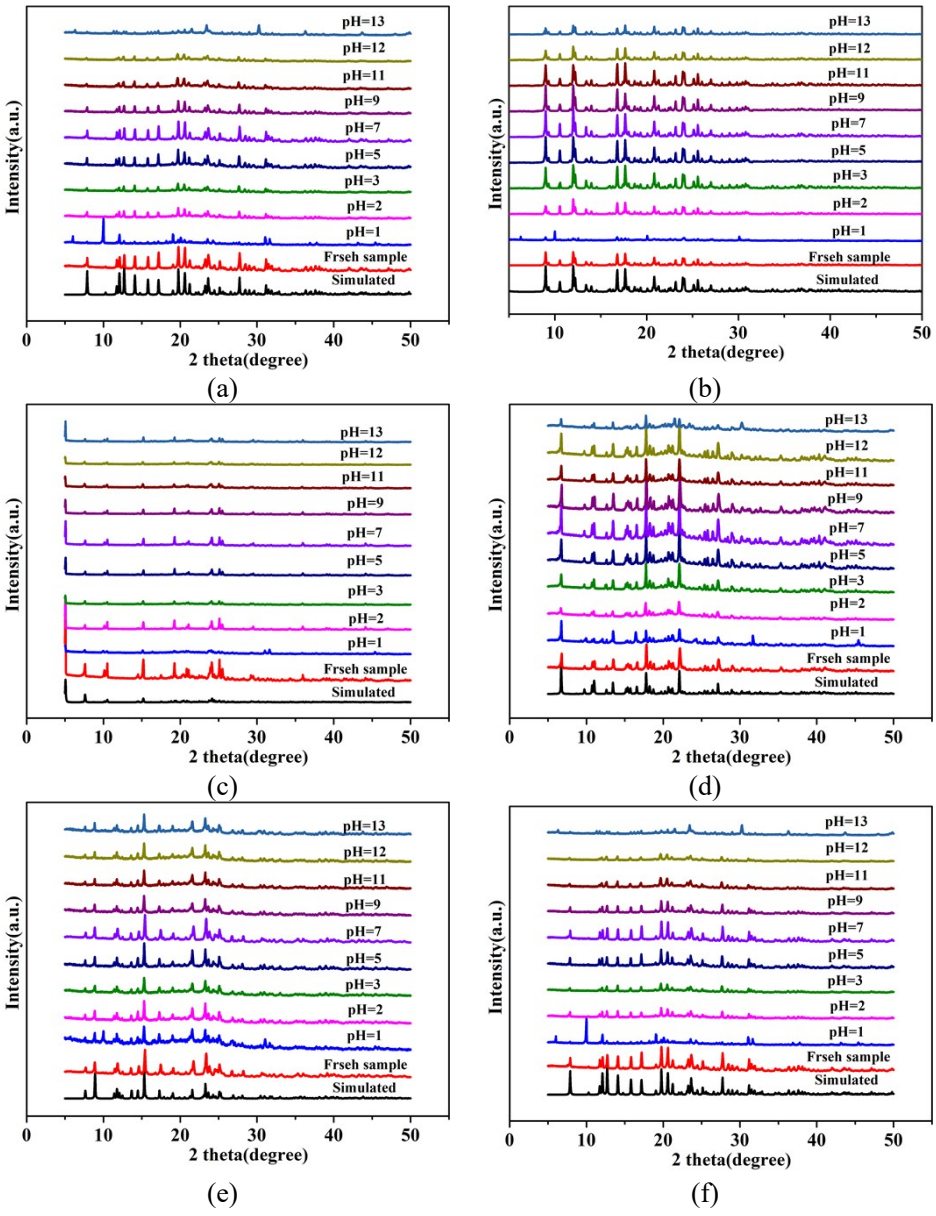

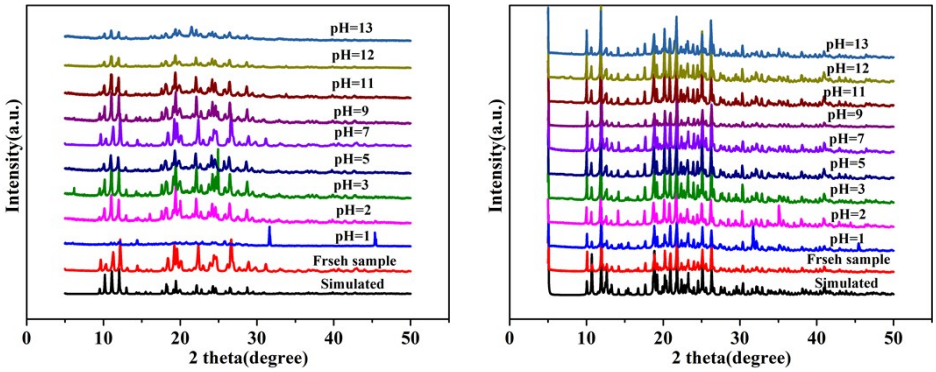

Fig. S4 The PXRD patterns of **1**–**8** after being soaked in acidic and basic aqueous solution in an extensive pH range of 2.0~13.0 for 24 h

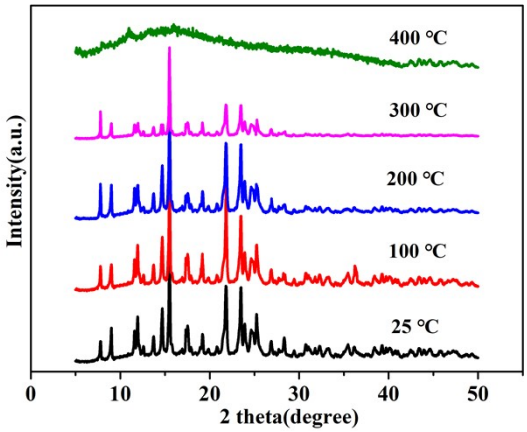

Fig. S5 The variable-temperature powder X-ray diffraction of CP **5**.

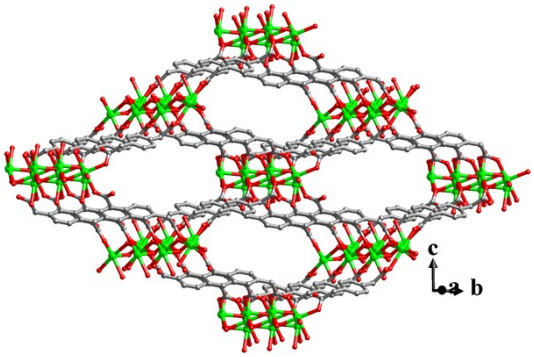

Fig. S6 View of the 3D frame work of **6**.

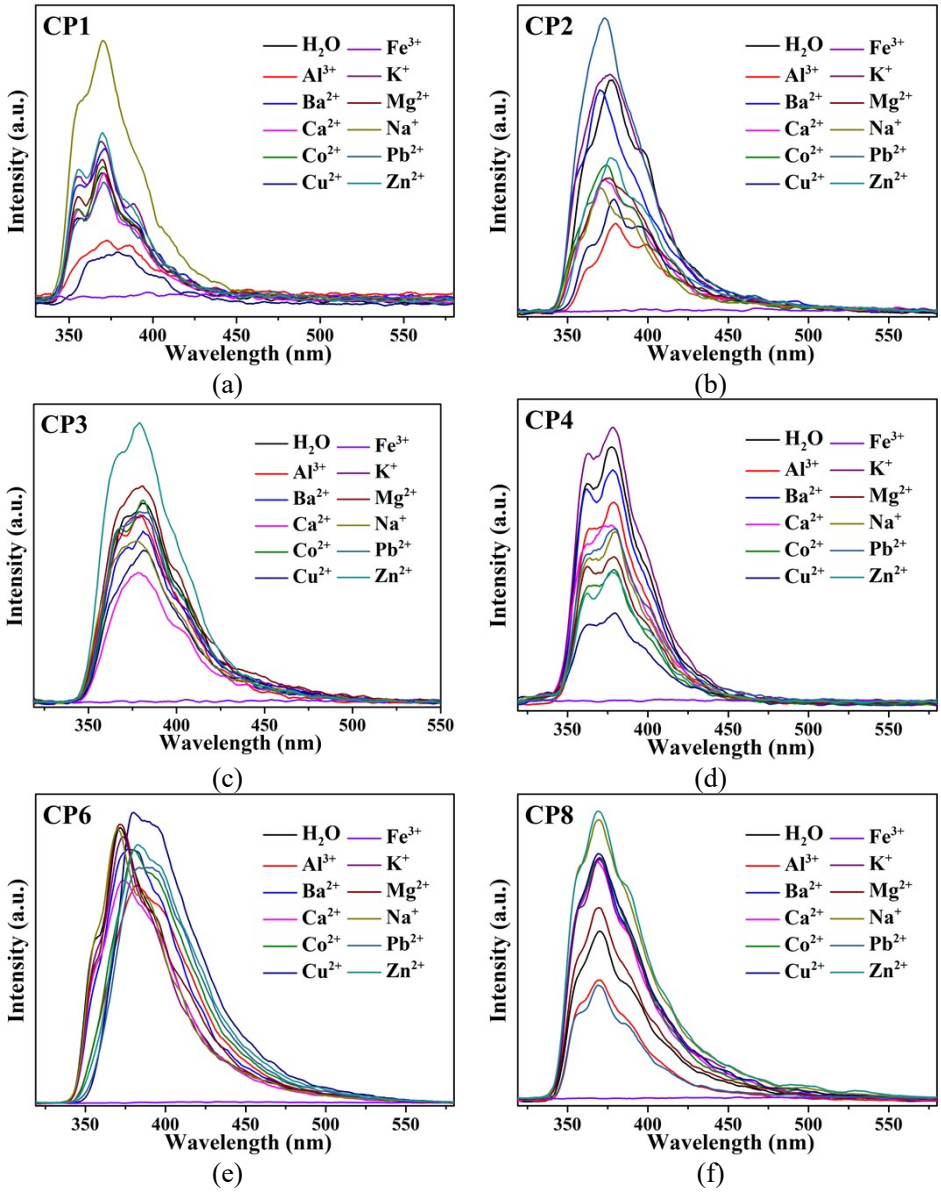

Fig. S7 Fluorescence emission intensity of **1**–**4**, **6** and **8** in different metal solutions.

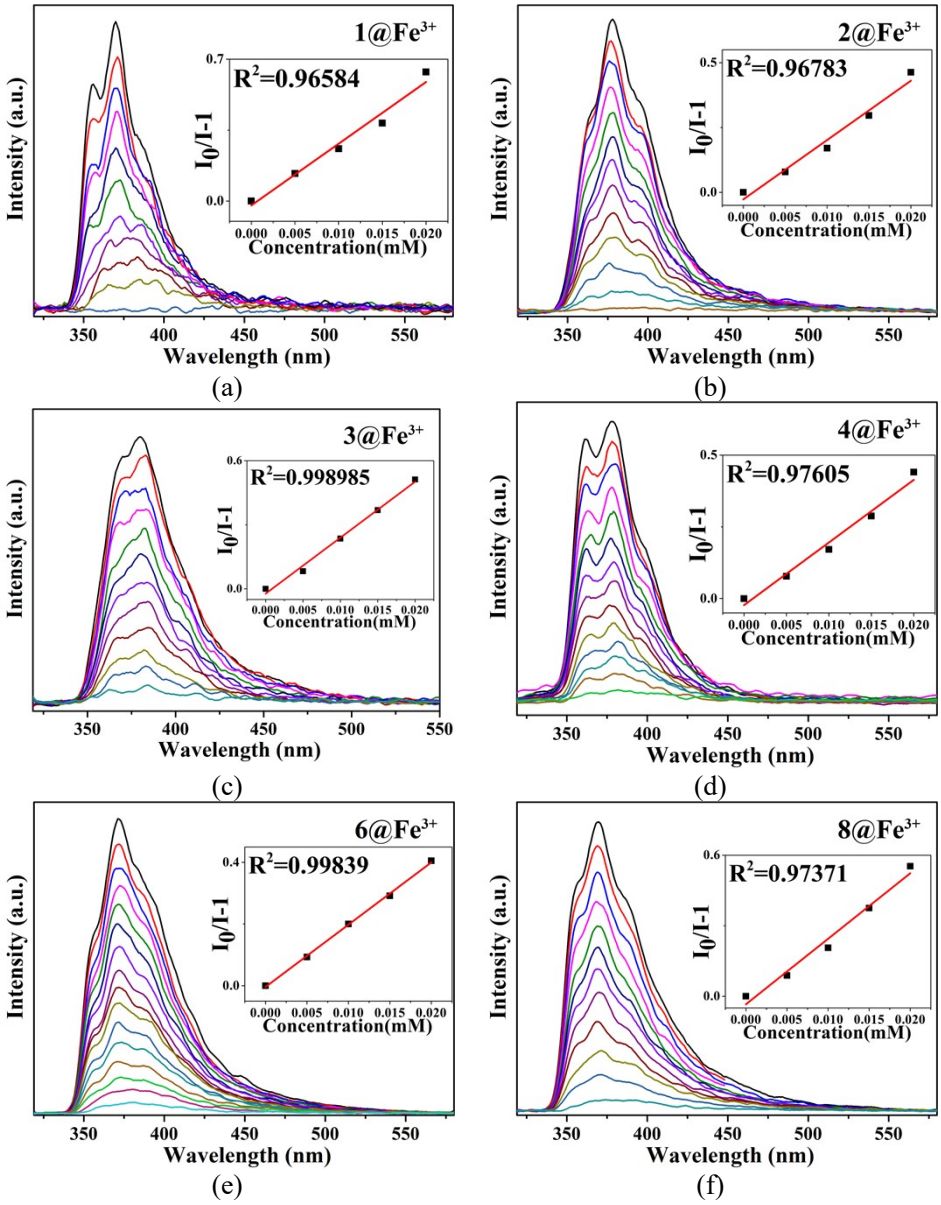

Fig. S8 Luminescence intensity of **1**–**4**, **6** and **8** upon the addition of Fe^{3+} ions in water.

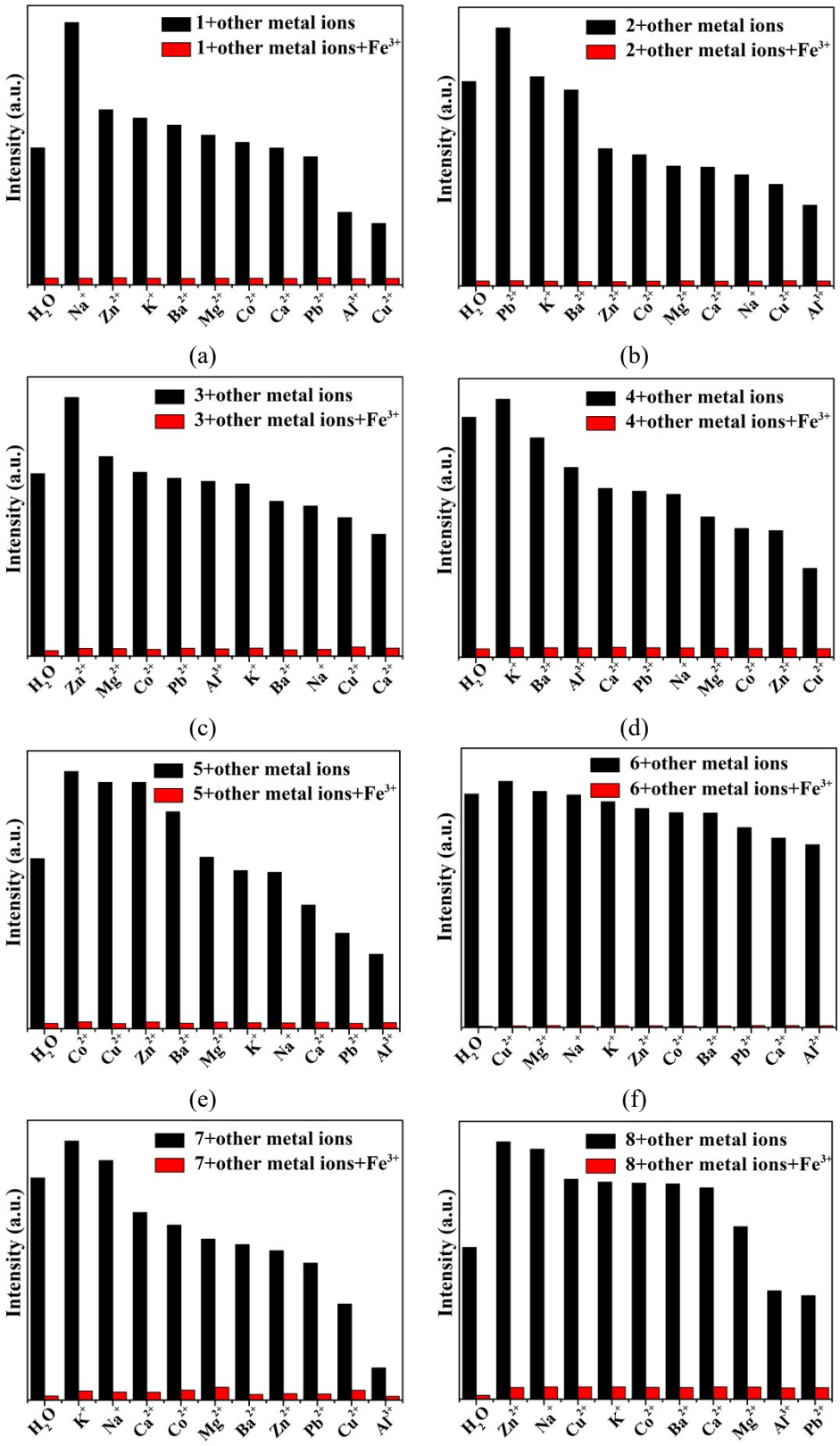

Fig. S9 Fluorescence emission intensities of **1**–**8** at room temperature upon the addition of Fe^{3+} or Fe^{3+} + interference mental ions.

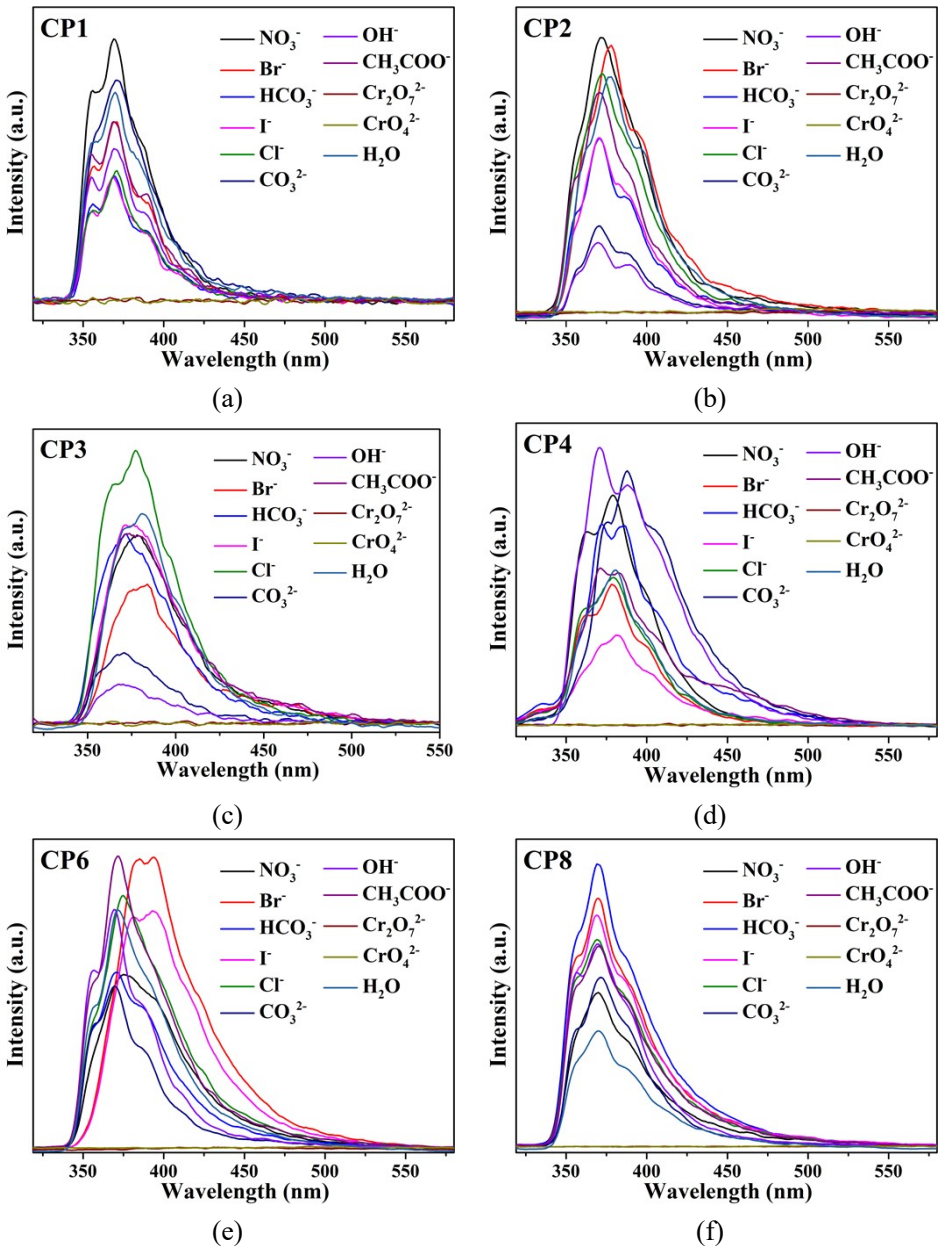

Fig. S10 Fluorescence emission intensity of **1**–**4**, **6** and **8** in different inorganic anions solutions.

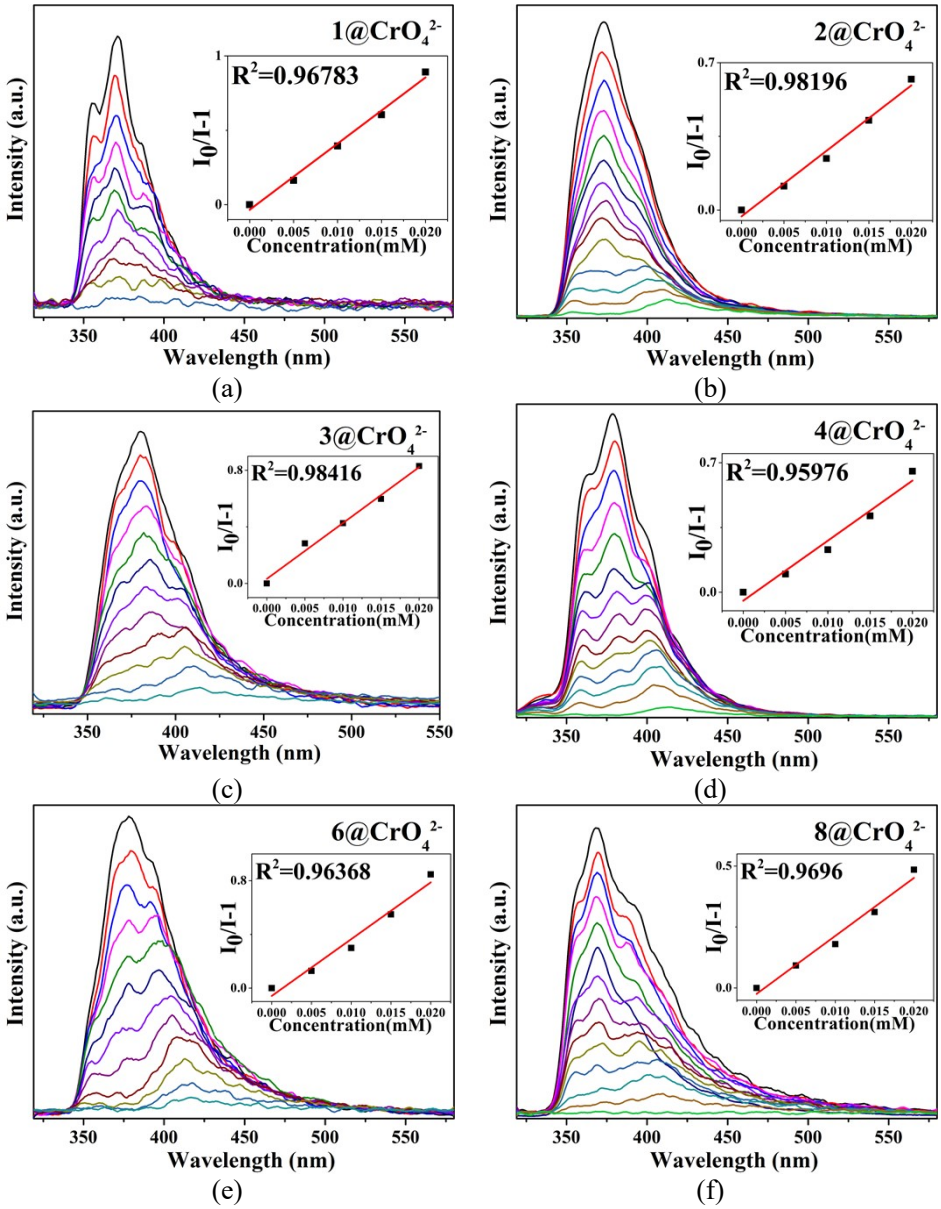

Fig. S11 Luminescence intensity of 1–4, 6 and 8 upon the addition of CrO_4^{2-} ions in water.

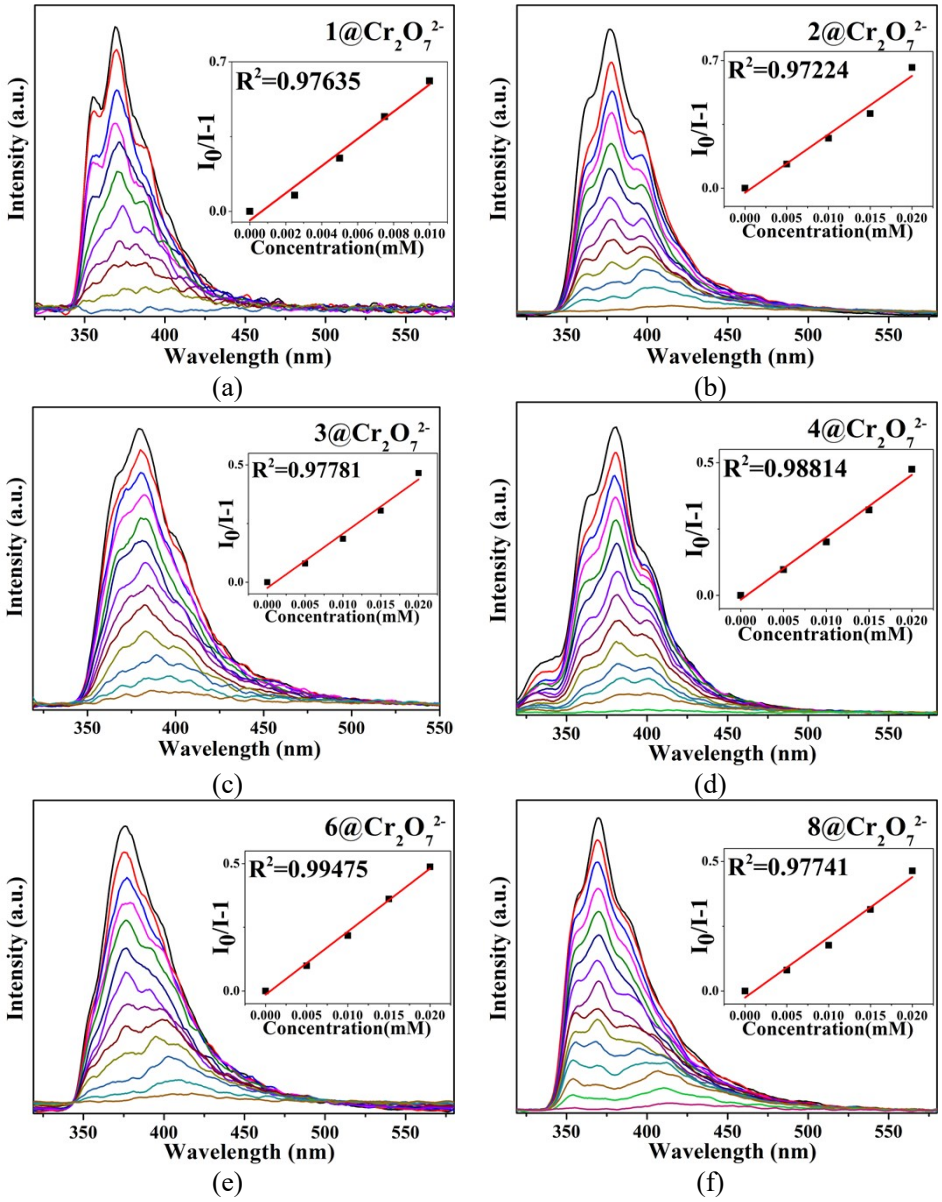

Fig. S12 Luminescence intensity of **1**–**4**, **6** and **8** upon the addition of $Cr_2O_7^{2-}$ ions in water.

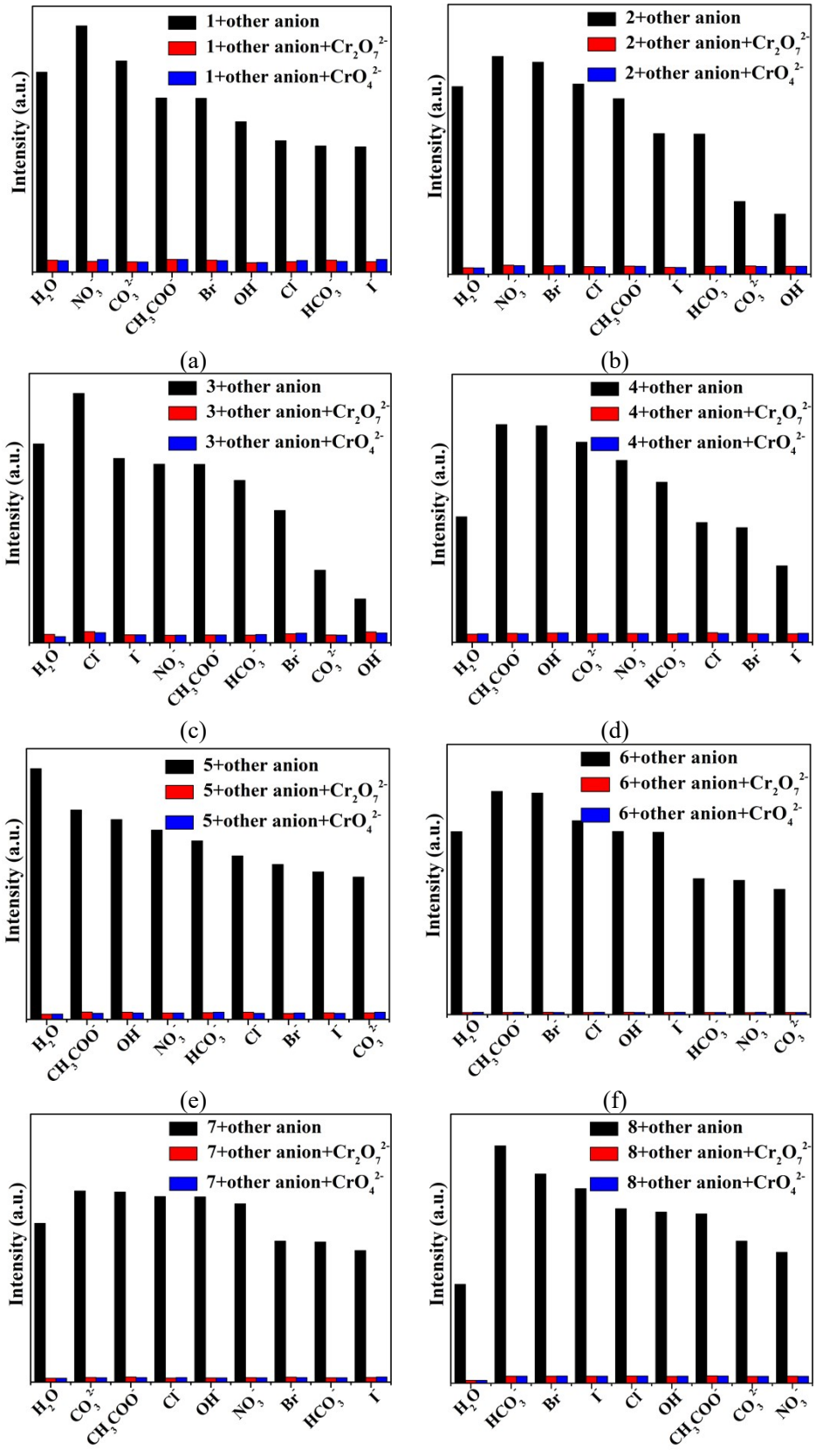

Fig. S13 Fluorescence emission intensities of **1**–**8** at room temperature upon the addition of CrO_4^{2-} and $Cr_2O_7^{2-}$ or CrO_4^{2-} and $Cr_2O_7^{2-}$+ interference inorganic anions.

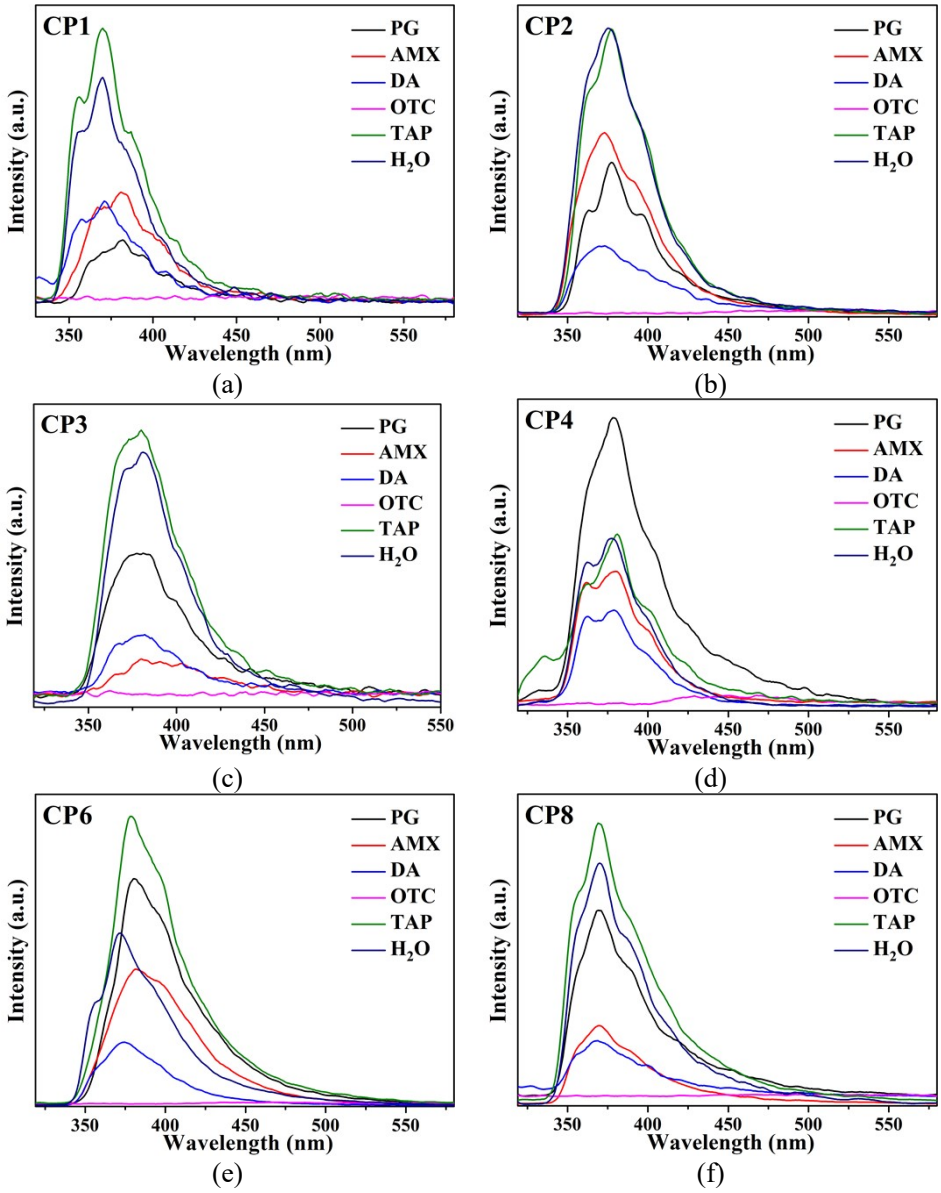

Fig. S14 Fluorescence emission intensity of **1**–**4**, **6** and **8** in different antibiotic solutions.

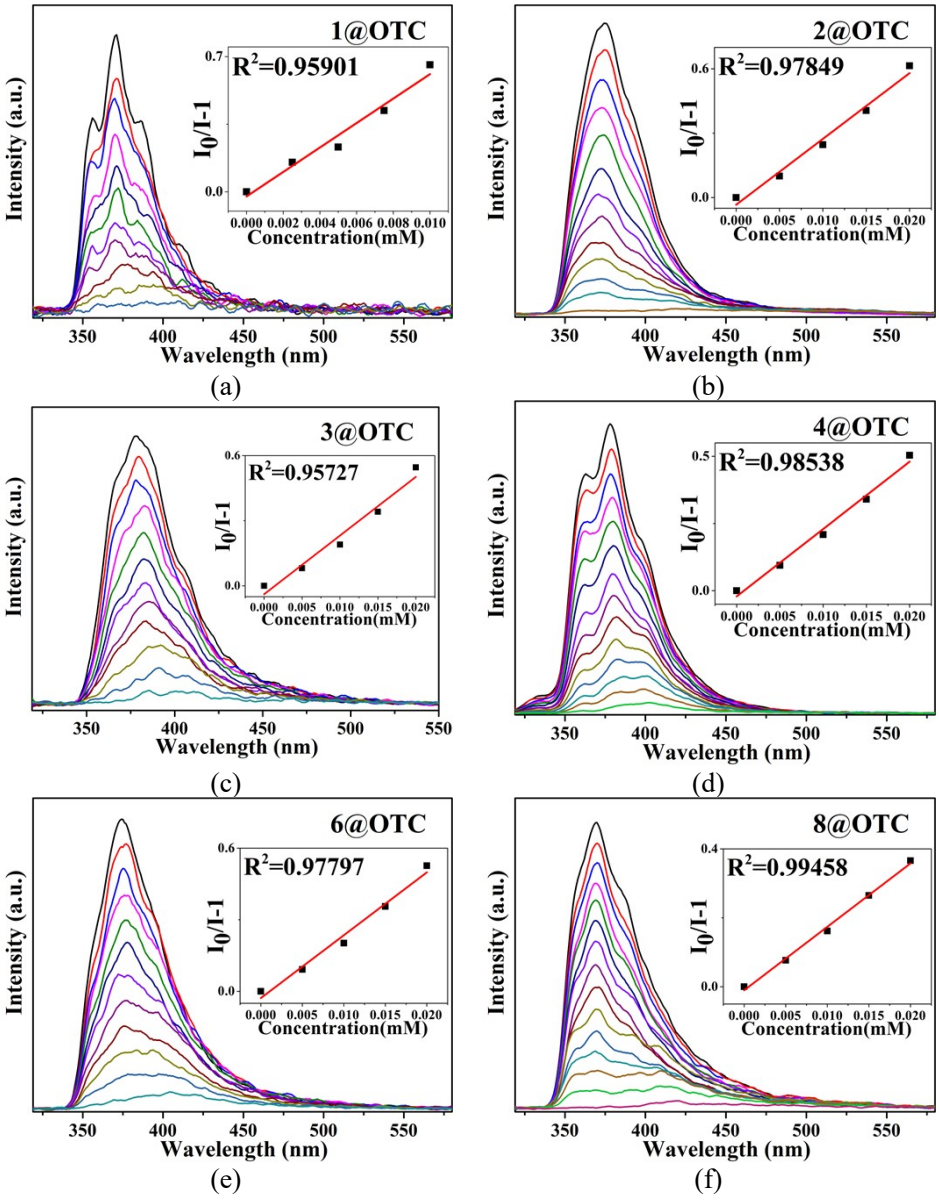

Fig. S15 Luminescence intensity of **1**–**4**, **6** and **8** upon the addition of antibiotic in water.

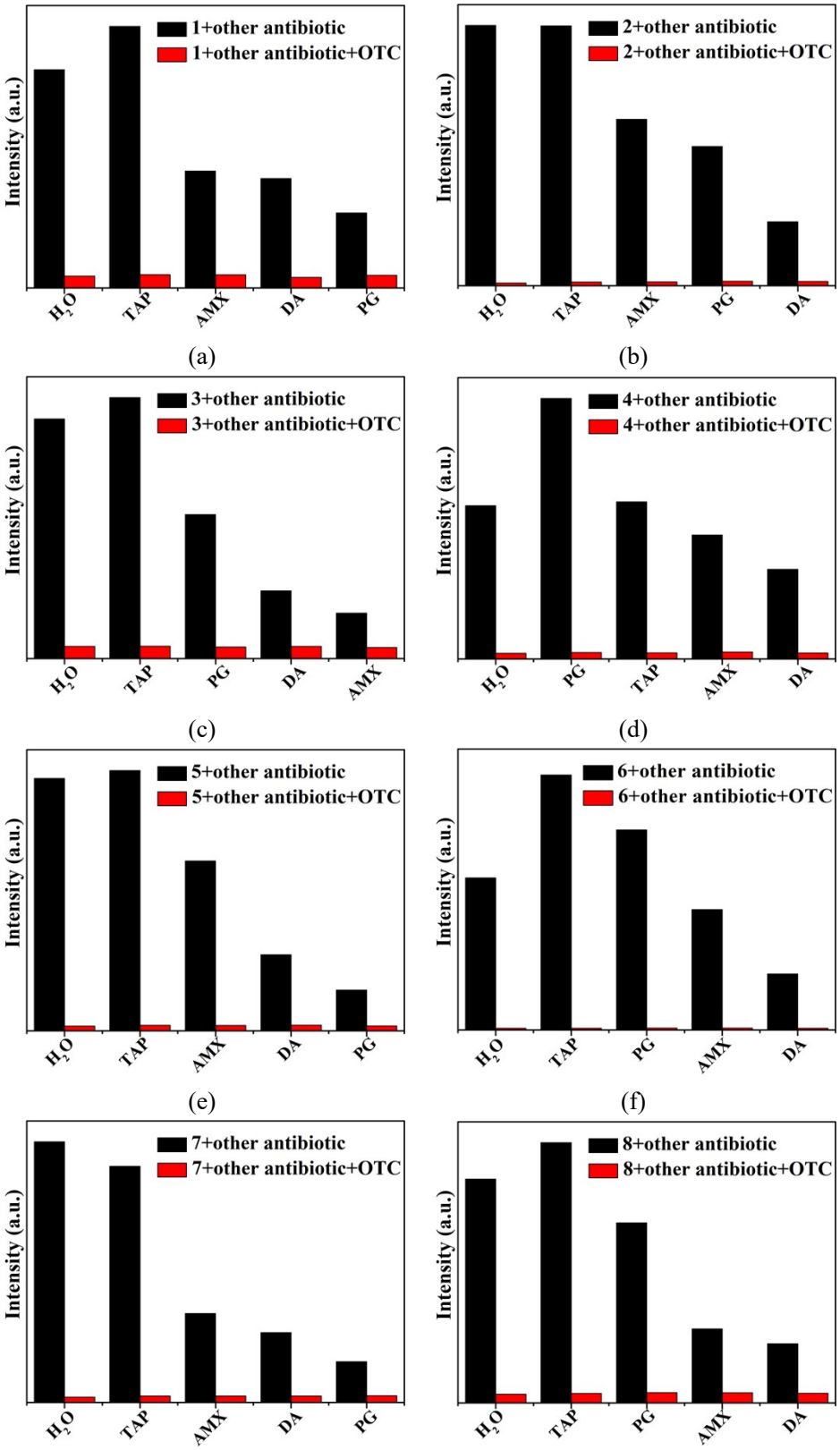

Fig. S16 Fluorescence emission intensities of **1**–**8** at room temperature upon the addition of OTC and OTC + interference inorganic anions.

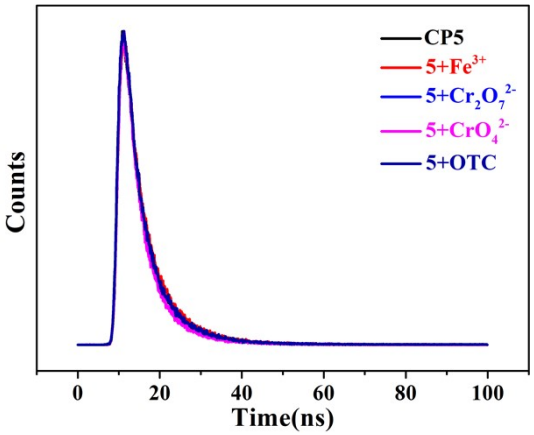

Fig. S17 Lifetime decay curves of CP **5** before and after the addition of four analyses.

Chart S1 The structural details of complexes **1**–**4**. (a) The carboxylic acids. (b) The coordination modes of central metals. (c) (c) The coordination modes of carboxylates. (d) The coordination modes of 4-bmnpd. (e) The schematic view of the structures **1**–**4**.

	1	**2**	**3**	**4**
(a)	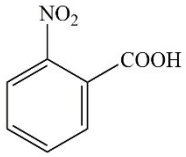	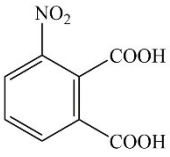	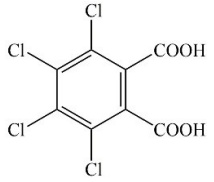	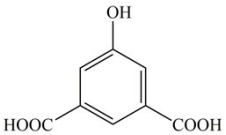
(b)	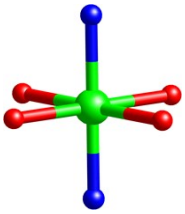	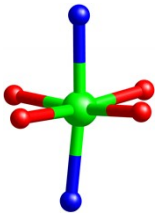	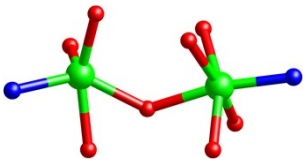	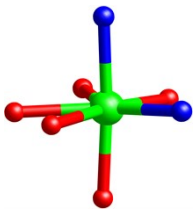
(c)	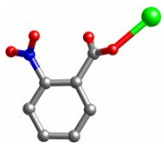	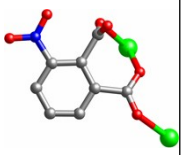	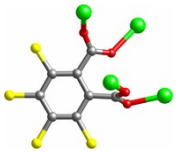	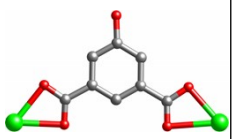
(d)	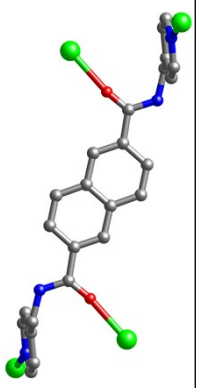	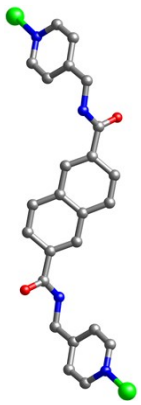	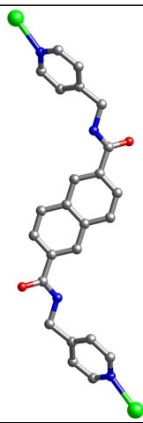	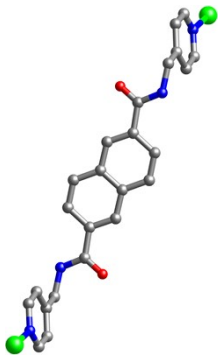
(e)	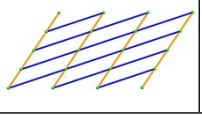	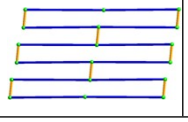	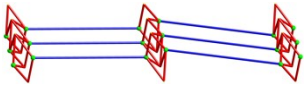	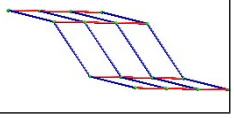

Chart S2 The structural details of complexes **5**–**8**. (a) The carboxylic acids. (b) The coordination modes of central metals. (c) The coordination modes of carboxylates. (d) The coordination modes of 4-bmnpd. (e) The schematic view of the structures **5**–**8**.

	5	**6**	**7**	**8**
(a)	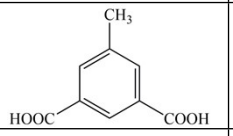	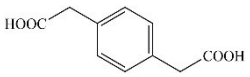	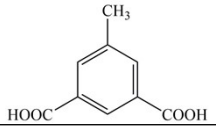	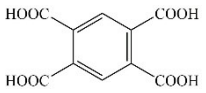
(b)	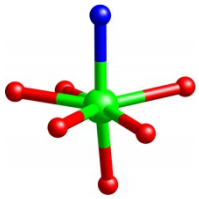	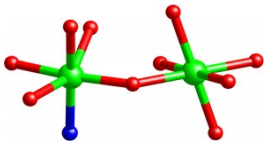	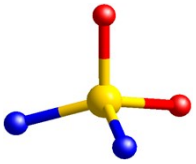	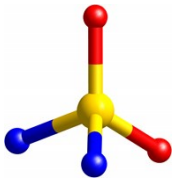
(c)	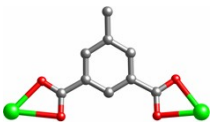	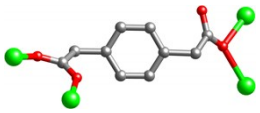	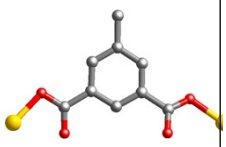	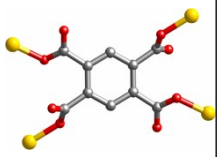
(d)	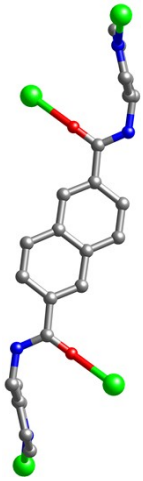	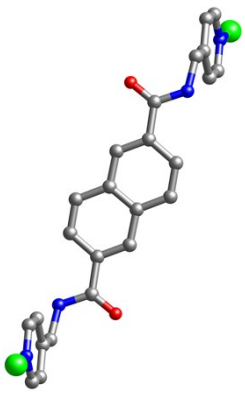	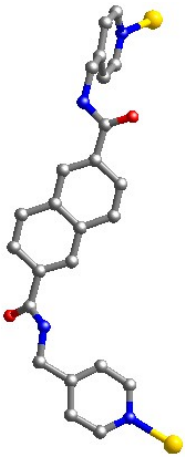	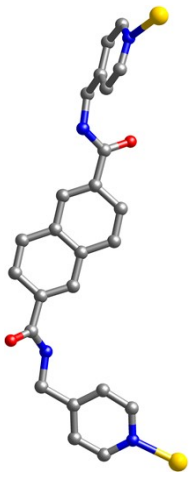
(e)